

Suppression of Rayleigh-Taylor instability in a gas-liquid standing-wave thermoacoustic engine

Jiaqi Luo
Institute of Refrigeration and
Cryogenics
Zhejiang University
Hangzhou 310027, China
11827052@zju.edu.cn

Qiang Zhou
Institute of Refrigeration and
Cryogenics
Zhejiang University
Hangzhou 310027, China
qiangz@zju.edu.cn

Tao Jin
Institute of Refrigeration and
Cryogenics
Zhejiang University
Hangzhou 310027, China
jintao@zju.edu.cn

Abstract—Gas-liquid thermoacoustic engine, using gas as working fluid and liquid as phase-matching element, can operate at a lower heat source temperature than the gas-only thermoacoustic engine, which is attractive for low-grade heat recovery. Rayleigh-Taylor instability, which is induced when a low-density fluid accelerates a high-density fluid, can occur in gas-liquid thermoacoustic engine. In this work, cylindrical or spherical floats with different dimensions were employed to suppress the Rayleigh-Taylor instability in a gas-liquid standing-wave thermoacoustic engine. Comparison between the onset and damping temperature differences obtained from the conditions with or without float was conducted to analyze the effects of instability on the onset and damping processes. The experimental results show that the dimension of float has marked effects on the onset and damping temperature differences, and there exists an optimal dimension for both cylindrical and spherical floats to achieve the lowest onset and damping temperature differences. After installing the float, the maximum decreases in the onset and damping temperature differences are 19.0% and 21.8%, respectively. This work demonstrates that the suppression of Rayleigh-Taylor instability by the suitably sized float can reduce the onset and damping temperature differences of a gas-liquid standing-wave thermoacoustic engine for low-grade heat recovery.

Keywords—gas-liquid thermoacoustic engine, low-grade heat, Rayleigh-Taylor instability, float, onset and damping temperature differences

I. INTRODUCTION

Utilization of low-grade heat has attracted considerable attention as a promising way for relieving growing global energy demands and reducing greenhouse-gas emissions [1]. Various alternative technologies capable of harvesting the low-grade heat have been proposed, such as organic Rankine cycle power generation [2], adsorption refrigeration [3], and thermoelectric generator [4]. Thermoacoustic engine has also attracted much interest thanks to its outstanding features of no moving component, high reliability and environmental benignity [5].

Onset and damping processes are fundamental phenomena in thermoacoustic engines [6,7], where the onset temperature

difference is the lowest temperature difference to trigger thermoacoustic oscillation, while the damping temperature difference is the lowest temperature difference to maintain thermoacoustic oscillation. Since the onset and damping temperature differences are critical parameters for the application of thermoacoustic engines to recover low-grade heat, many efforts have been devoted to decrease the onset and damping temperature differences of thermoacoustic engines. One of the effective methods is to introduce liquid column into a gas-only thermoacoustic engine, and a series of numerical and experimental studies on the gas-liquid thermoacoustic engines have been conducted [8–10]. Tang et al. [8] numerically and experimentally analyzed the effect of liquid on onset temperature difference and found that the liquid with low kinematic viscosity was preferable for low onset temperature difference. Luo et al. [9] analyzed the effect of working gas on the onset temperature difference of a gas-liquid traveling-wave thermoacoustic engine, where helium, nitrogen and carbon dioxide were selected as working gas, respectively. Their experimental results showed that carbon dioxide was preferable for achieving a low onset temperature difference. Biwa et al. [10] studied the effects of liquid column on the phasing difference between pressure and velocity and on the specific acoustic impedance in the regenerator, and found that the liquid column can increase the specific acoustic impedance while keeping the traveling wave phasing in the regenerator to achieve a low onset temperature difference.

Rayleigh-Taylor instability can be induced when a low-density fluid accelerates a high-density fluid [11], and can occur in a gas-liquid thermoacoustic engine. Biwa et al. [12] employed two methods to suppress the Rayleigh-Taylor instability in a gas-liquid traveling-wave thermoacoustic engine, i.e., the enlargement of tube cross-sectional area and the installation of a submerged float. Their experimental results showed that these methods could successfully suppress the instability of free liquid surface and increase the pressure amplitude by almost twice of the original condition. Besides, the results also indicated that the onset temperature difference did not change significantly after suppressing the instability. However, the present work shows that the suppression of the Rayleigh-Taylor instability in a gas-liquid standing-wave thermoacoustic engine using the submerged float can have marked effects on both onset and damping temperature differences.

In this work, the cylindrical or spherical floats with different dimensions are employed to suppress the Rayleigh-Taylor instability in gas-liquid standing-wave thermoacoustic engine. The onset and damping temperature differences obtained from the conditions with or without float are compared to analyze the effects of instability on the onset and damping processes of the gas-liquid standing-wave thermoacoustic engine.

II. EXPERIMENTAL SYSTEM

A. Configuration of gas-liquid standing-wave thermoacoustic engine

A gas-liquid standing-wave thermoacoustic engine with symmetrical configuration is shown in Fig. 1. The engine is composed of two sets of hot buffer, tapered tube, hot tube, heater, stack and cooler, and a U-shaped tube containing liquid column. As shown in Fig. 1, the heat transfer blocks inside the heater and cooler are both of fin type and made of copper. The fin spacing and the fin width are 0.0015 m and 0.001 m, respectively. The stack is composed of a number of stainless steel slices with a thickness of 0.001 m. The slice is manufactured into finned structure by spark-erosion wire cutting, with a fin spacing 0.0015 mm and a fin width 0.0007 m. Table I lists the dimensions of main components in the gas-liquid standing-wave thermoacoustic engine, where the hydraulic radius is defined as the ratio of the channel's cross-sectional area to its perimeter, and the porosity is defined as the ratio of the volume of fluid to the total volume of porous medium.

B. Polyethylene float

To suppress the instability of free liquid surface, a float is installed at each side of the liquid column. The float is made of ultra-high-molecular-weight polyethylene, and its density is around 950 kg/m³, which is close to the density of water, so that it can follow the oscillation of water. Eleven types of float indexed from A to K are employed in the experiments, whose dimensions are listed in Table II. Limited by the diameter of U-shaped tube (i.e., 0.056 m), the maximum diameter of cylindrical or spherical float is selected as 0.055 m.

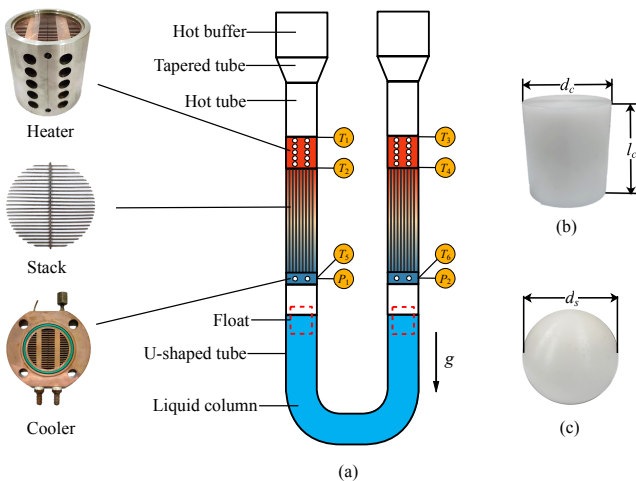


Fig. 1. Schematic of the gas-liquid standing-wave thermoacoustic engine (a), where cylindrical (b) or spherical (c) polyethylene float is employed to suppress the instability of free liquid surface.

TABLE I. DIMENSIONS OF MAIN COMPONENTS IN THE GAS-LIQUID STANDING-WAVE THERMOACOUSTIC ENGINE.

Component	Diameter (m)	Length (m)	Hydraulic radius (m)	Porosity
Hot buffer	0.14	0.210	0.035	1
Tapered tube	–	0.072	–	1
Hot tube	0.056	0.215	0.014	1
Heater	0.056	0.064	0.00075	0.331
Stack	0.056	0.300	0.00075	0.675
Cooler	0.056	0.020	0.00075	0.440
U-shaped tube	0.056	0.904	0.014	1
Liquid column	0.056	0.670	0.014	1

TABLE II. DIMENSIONS OF DIFFERENT CYLINDRICAL AND SPHERICAL POLYETHYLENE FLOATS.

Float	Diameter (m)	Length (m)
Cylindrical float	Float A	0.051
	Float B	0.053
	Float C	0.055
	Float D	0.055
	Float E	0.055
	Float F	0.055
Spherical float	Float G	0.035
	Float H	0.040
	Float I	0.045
	Float J	0.050
	Float K	0.055

C. Measurement and error analysis

As displayed in Fig. 1, three K-type thermocouples (CHINO 1SCHS1 series, with the accuracies of $\pm 1.1^\circ\text{C}$) are employed to measure the temperatures of heater and cooler, where two thermocouples are separately installed at the top and bottom of the heater, and another thermocouple is installed at the cooler. The temperatures of two heaters are controlled to be the same by changing the electric power inputs of the cartridge heaters. The electric power input is measured by an electric power meter (Weibo PF1200). The temperatures of two coolers are kept at around 300 K by circulating water. The average of T_1 , T_2 , T_3 and T_4 is regarded as the hot temperature, and the average of T_5 and T_6 is regarded as the cold temperature. A pressure sensor (GE UNIK 5000 series, with the accuracies of 0.04% FS) is installed at the cooler. The temperature signals are acquired by an Agilent 34970A data acquisition switch unit with an Agilent 34901A 20-channel multiplexor module, and the pressure signals are acquired by an NI 9205 analog input module. All the signals are displayed and recorded in a computer through the self-coded LABVIEW program.

The measurement error σ_{me} , containing systematic error σ_{se} and random error σ_{re} , can be expressed as [13]

$$\sigma_{me} = \sqrt{\sigma_{se}^2 + \sigma_{re}^2} \quad (1)$$

where σ_{se} mainly depends on the accuracy of measuring instruments, and σ_{re} can be written as

$$\sigma_{re} = \sqrt{\frac{\sum_{j=1}^n (y_j - \bar{y})^2}{n-1}} \quad (2)$$

where y_j represents the measured data of the j th measurement, n is the times of repeated measurement. According to Eqs. (1) and (2), the maximum measurement errors of temperature and resonance frequency are ± 1.1 K and ± 0.0075 Hz, respectively.

III. EXPERIMENTAL PROCEDURE

In the experiments, onset and damping processes of the gas-liquid standing-wave thermoacoustic engine are studied, during which the onset and damping temperature differences are measured. The onset temperature difference is measured through adjusting the electric power inputs to the cartridge heaters, with a temperature elevation speed at the heater lower than $0.5^\circ\text{K}/\text{min}$, where the hot-cold temperature difference at the moment of oscillation initiation is regarded as the onset temperature difference. After the occurrence of onset process, the heater is kept heated for a period of time, and then the input power is adjusted to zero for analyzing the damping process. The hot-cold temperature difference at which the oscillation completely vanishes is regarded as the damping temperature difference.

The entire evolution of pressure amplitude with the hot-cold temperature difference is displayed in Fig. 2. At the beginning, the pressure amplitude maintains around zero with the increase of hot-cold temperature difference. When the hot-cold temperature difference exceeds a certain value, the pressure amplitude experiences a sudden rise, indicating the occurrence of onset. The critical hot-cold temperature difference is regarded as the onset temperature difference, which is 82 K for the illustrative case. The heat exchange between the heater and the working gas is strengthened by the increased pressure amplitude, and the hot-cold temperature difference begins to decrease after the onset. After a period of time when the pressure amplitude tends to stabilize, the input power is turned off, resulting in further decrease of hot-cold temperature difference and pressure amplitude. When the hot-cold temperature difference drops to 51 K, the oscillation completely vanishes, and then 51 K is considered as the damping temperature difference. The damping temperature difference is lower than the onset temperature difference, and a hysteric loop was observed during the onset and damping processes in the gas-liquid standing-wave thermoacoustic engine. Similar phenomenon has also been detected in other types of thermoacoustic engine [6,7].

IV. RESULTS AND DISCUSSION

Experiments have been carried out on the gas-liquid standing-wave thermoacoustic engine, where the nitrogen of 1 MPa is selected as the working gas, and water is chosen as the liquid column. Three different conditions, i.e., without float, with cylindrical float and with spherical float, are studied, focusing on the onset and damping temperature differences.

A. Cylindrical float

Fig. 3 presents the variation of onset temperature difference ΔT_{onset} , damping temperature difference $\Delta T_{\text{damping}}$ and onset resonance frequency f_{onset} with the diameter of

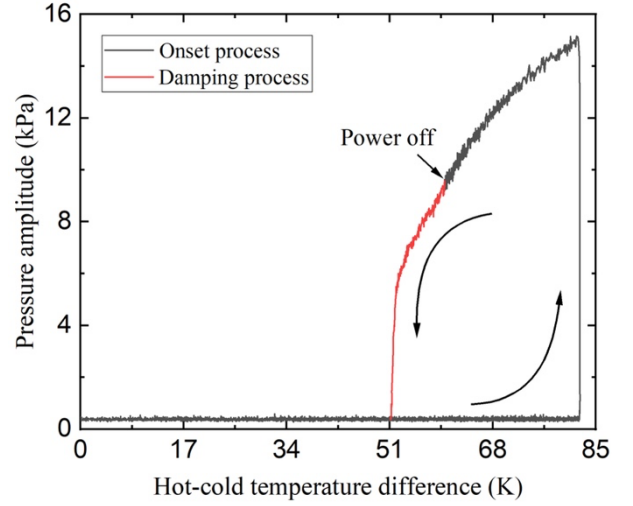


Fig. 2. Evolution of pressure amplitude with hot-cold temperature difference during onset and damping processes.

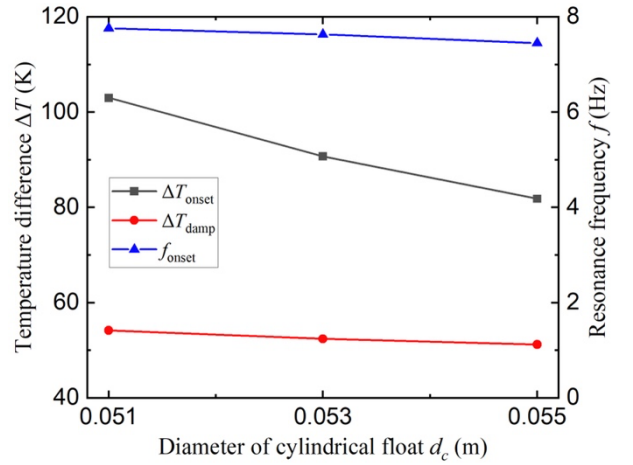


Fig. 3. Onset temperature difference, damping temperature difference and onset resonance frequency with different diameters of the cylindrical float, where the length is kept at 0.050 m.

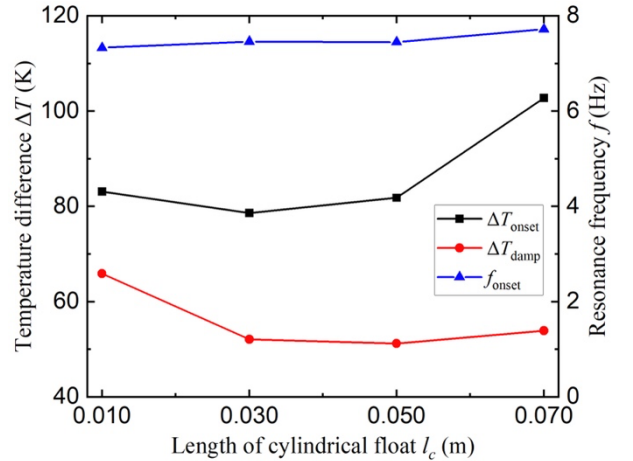


Fig. 4. Onset temperature difference, damping temperature difference and onset resonance frequency with different lengths of the cylindrical float, where the diameter is 0.055 m.

cylindrical float d_c , where the length of cylindrical float l_c is fixed at 0.050 m. Since the cylindrical float with larger diameter is preferable to suppress the Rayleigh-Taylor instability [12], ΔT_{onset} decreases with the increase of d_c and reaches the lowest value when d_c equals to 0.055 m. $\Delta T_{\text{damping}}$

decreases slightly with the increase of d_c , indicating that $\Delta T_{\text{damping}}$ is insensitive to d_c within the investigated range. In the experiments, the charging pressure is fixed at 1 MPa, while the mean pressure when the onset process occurs is higher than 1 MPa due to the increased mean temperature. Since a higher mean pressure results in a higher sound speed and then a higher resonance frequency, f_{onset} has similar trend to ΔT_{onset} and decreases with the increase of d_c .

Fig. 4 presents the effects of l_c on ΔT_{onset} , $\Delta T_{\text{damping}}$ and f_{onset} , where d_c is 0.055 m. Since the cylindrical float with longer length is preferable to suppress the Rayleigh-Taylor instability [12], ΔT_{onset} and $\Delta T_{\text{damping}}$ decrease when l_c increases from 0.010 m to 0.030 m. However, when l_c increases from 0.050 m to 0.070 m, ΔT_{onset} and $\Delta T_{\text{damping}}$ increase instead, which can be attributed to the rise in friction loss between the float and the tube wall. Therefore, an optimal l_c exists for achieving the lowest ΔT_{onset} and $\Delta T_{\text{damping}}$, where the lowest ΔT_{onset} is obtained at l_c of 0.030 m and the lowest $\Delta T_{\text{damping}}$ is obtained at l_c of 0.050 m.

As declared in [12], the installation of cylindrical float to suppress the Rayleigh-Taylor instability did not significantly affect ΔT_{onset} of a gas-liquid travelling-wave thermoacoustic engine. However, the experimental results in the present work show that ΔT_{onset} of the gas-liquid standing-wave thermoacoustic engine can be affected after installing cylindrical float. Besides, the dimension of cylindrical float has marked effects on ΔT_{onset} and $\Delta T_{\text{damping}}$, where the maximum differences in ΔT_{onset} and $\Delta T_{\text{damping}}$ can reach 24 K and 15 K, respectively. Therefore, the installation of suitably sized cylindrical float to suppress the Rayleigh-Taylor instability is important for the gas-liquid standing-wave thermoacoustic engine to achieve low onset and damping temperature differences.

B. Spherical float

Spherical float is also employed to suppress the instability of the free liquid surface. Five spherical floats with different diameters d_s are installed, and the corresponding ΔT_{onset} , $\Delta T_{\text{damping}}$ and f_{onset} are displayed in Fig. 5. Compared to the results with cylindrical float, the installation of spherical float can lead to a low ΔT_{onset} at a large range of d_s . Similar to cylindrical float, the dimension of spherical float can affect ΔT_{onset} and $\Delta T_{\text{damping}}$, where the maximum differences in ΔT_{onset} and $\Delta T_{\text{damping}}$ are 14 K and 7 K, respectively. The minimum ΔT_{onset} is obtained at d_s of 0.045 m, and the minimum $\Delta T_{\text{damping}}$ is obtained at d_s of 0.055 m. The variation of f_{onset} with d_s is similar to that of ΔT_{onset} , and the minimum f_{onset} is obtained when d_s equals to 0.045 m where ΔT_{onset} is the lowest.

C. Comparison between the results with and without floats

Fig. 5 depicts the relative deviations of ΔT_{onset} and $\Delta T_{\text{damping}}$ obtained from the condition with float to those obtained from the condition without float, where the negative value indicates that the corresponding value from the condition with float is smaller than that from the condition without float. It is found that the installation of float is not always beneficial to decrease ΔT_{onset} and $\Delta T_{\text{damping}}$. Besides, the decrease in ΔT_{onset} does not mean the decrease in $\Delta T_{\text{damping}}$, and vice versa. With the exception of the floats A, D and F, both ΔT_{onset} and $\Delta T_{\text{damping}}$ are decreased after installing float. The maximum decrease in ΔT_{onset} is 19.0% using the float E, and the maximum decrease in $\Delta T_{\text{damping}}$ is 21.8% using the float C. Furthermore, compared

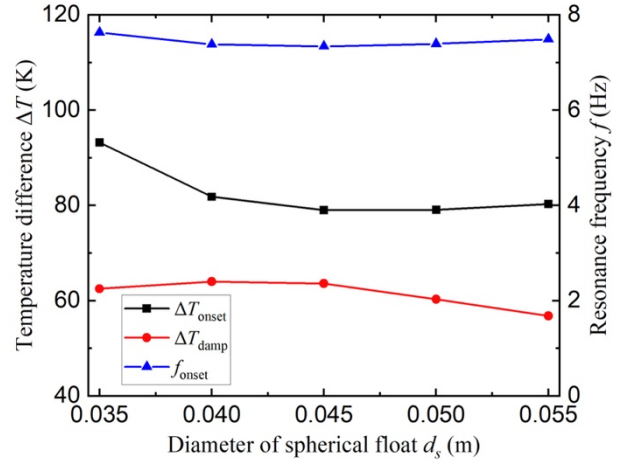


Fig. 5. Onset and damping temperature differences, and onset resonance frequency with different diameters of the spherical float.

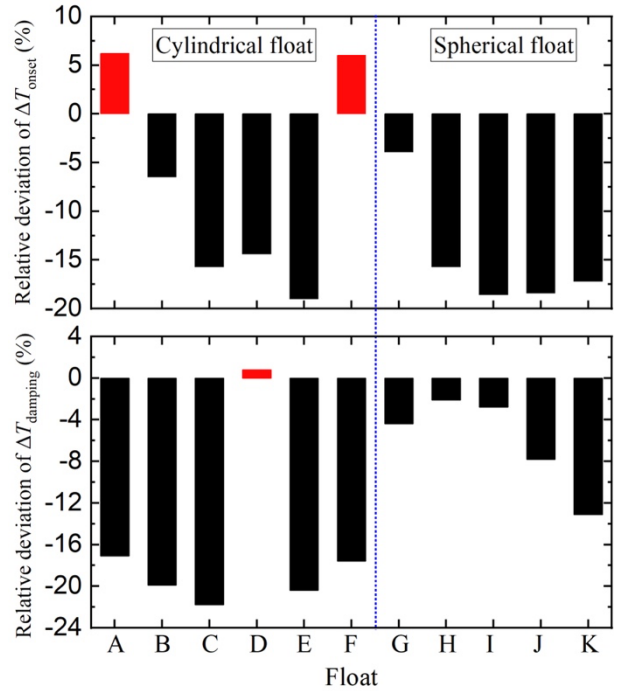


Fig. 6. Relative deviations of onset and damping temperature differences obtained from conditions with or without float.

with spherical float, the cylindrical float is preferable to reduce ΔT_{onset} and $\Delta T_{\text{damping}}$. The maximum decrease in ΔT_{onset} is 19.0% and 18.6% for cylindrical and spherical floats, respectively, and the maximum decrease in $\Delta T_{\text{damping}}$ is 21.8% and 13.1% for cylindrical and spherical floats, respectively. Nevertheless, the suitably sized cylindrical or spherical float should be used to decrease ΔT_{onset} and $\Delta T_{\text{damping}}$.

V. CONCLUSION

In this work, cylindrical or spherical floats with different dimensions are employed to suppress the Rayleigh-Taylor instability in a gas-liquid standing-wave thermoacoustic engine. The onset and damping temperature differences obtained from the working conditions with or without float are compared, based on which the effects of instability on the onset and damping temperature differences are analyzed. Main conclusions are summarized as follows:

(1) The dimension of float has marked effects on onset and damping temperature differences. There exists an optimal

dimension for both cylindrical and spherical floats to obtain the lowest onset and damping temperature differences.

(2) The installation of suitably sized float to suppress the Rayleigh-Taylor instability can reduce the onset and damping temperature differences. Compared to the results without float, the maximum decrease in onset temperature difference is 19.0% using cylindrical float with a length of 0.030 m and a diameter of 0.055 m, and the maximum decrease in damping temperature difference is 21.8% using cylindrical float with a length of 0.050 m and a diameter of 0.055 m.

(3) The installation of cylindrical float is preferable to obtain lower onset and damping temperature differences compared with spherical float, especially the damping temperature difference. The maximum decreases in damping temperature difference are 21.8% and 13.1% for cylindrical and spherical floats, respectively.

ACKNOWLEDGMENT

This work is financially supported by the Natural Science Foundation of Zhejiang Province (No. LZ20E060001) and the National Natural Science Foundation of China (No. 52176023).

REFERENCES

- [1] C. Forman, I.K. Muritala, R. Pardemann, and B. Meyer, "Estimating the global waste heat potential," *Renew. Sustain. Energy Rev.*, vol. 57, pp. 1568–1579, 2016.
- [2] J. Bao, and L. Zhao, "A review of working fluid and expander selections for organic Rankine cycle," *Renew. Sustain. Energy Rev.*, vol. 24, pp. 325–342, 2013.
- [3] D. Wang, J. Zhang, Q. Yang, N. Li, and K. Sumathy, "Study of adsorption characteristics in silica gel–water adsorption refrigeration," *Appl. Energy*, vol. 113, pp. 734–741, 2014.
- [4] S. Shittu, G. Li, X. Zhao, X. Ma, Y.G. Akhlaghi, and E. Ayodele, "High performance and thermal stress analysis of a segmented annular thermoelectric generator," *Energy Convers. Manag.*, vol. 184, pp. 180–193, 2019.
- [5] T. Jin, J. Huang, Y. Feng, R. Yang, K. Tang, and R. Radebaugh, "Thermoacoustic prime movers and refrigerators: Thermally powered engines without moving components," *Energy*, vol. 93, pp. 828–853, 2015.
- [6] G. Chen, and T. Jin, "Experimental investigation on the onset and damping behavior of the oscillation in a thermoacoustic prime mover," *Cryogenics*, vol. 39, pp. 843–846, 1999.
- [7] J. Tan, J. Wei, and T. Jin, "Onset and damping characteristics of a closed two-phase thermoacoustic engine," *Appl. Therm. Eng.*, vol. 160, pp. 114086, 2019. K. Tang, T. Lei, and T. Jin, "Influence of working liquid on the onset characteristics of a thermoacoustic engine with gas and liquid," *J. Appl. Phys.*, vol. 112, pp. 094909, 2012.
- [8] D. Li, Y. Chen, E. Luo, and Z. Wu, "Study of a liquid-piston traveling-wave thermoacoustic heat engine with different working gases," *Energy*, vol. 74, pp. 158–163, 2014.
- [9] H. Hyodo, S. Tamura, and T. Biwa, "A looped-tube traveling-wave engine with liquid pistons," *J. Appl. Phys.*, vol. 122, pp. 114902, 2017.
- [10] G. Taylor, "The instability of liquid surfaces when accelerated in a direction perpendicular to their planes. I," *Proc. R. Soc. Lond. Ser. Math. Phys. Sci.*, vol. 201, pp. 192–196, 1950.
- [11] P. Murti, H. Hyodo, and T. Biwa, "Suppression of liquid surface instability induced by finite-amplitude oscillation in liquid piston Stirling engine," *J. Appl. Phys.*, vol. 127, pp. 154901, 2020.
- [12] J.R. Taylor, "An Introduction to Error Analysis: the Study of Uncertainties in Physical Measurements," University Science Books, New York, 1997.